JOURNAL OF MATERIALS SCIENCE 30 (1995) 5743–5749

Synthesis of bulk nanocrystalline nickel by pulsed electrodeposition

A.M. EL-SHERIK, U. ERB
Department of Materials and Metallurgical Engineering, Queen's University, Kingston, Ontario, Canada K7L 3N6

Square-wave cathodic current modulation was used to produce nanocrystalline nickel electrodeposits with grain sizes in the range 40–10 nm from saccharin-containing Watts-type baths. The optimum plating conditions to synthesize nanocrystals, namely pulse on- and off-time and peak current density, as well as bath pH and temperature, were identified. At these plating conditions, the grain size of the electrodeposits was found to decrease with increasing saccharin concentration in the bath. The preferred orientation of the deposits progressively changed from a strong (2 0 0) fibre texture for a saccharin-free bath to a (1 1 1) (2 0 0) double fibre texture for a bath containing 10 g l^{-1} saccharin. Transmission electron microscopy showed that the electrodeposits consist of uniform structure with narrow grain-size distribution. These deposits, as expected, were found to contain co-deposited sulphur and carbon impurities.

1. Introduction

Electroplated nickel is used extensively in many engineering applications, ranging from simple thin film for decorative purposes and corrosion- and wear-resistant coatings to bulk electroformed products such as rotary printing cylinders [1]. Although electroplated nickel has been widely used for over a century now, considerable interest remains in improving its mechanical, electrical, magnetic and corrosion properties. These properties are strongly influenced by many parameters such as composition, morphology, internal stresses, preferred orientation and grain size of the deposits [1].

In recent years, as a result of advances in the understanding of the effects of grain boundaries on the structure and properties of materials, structures with grain sizes less than 100 nm have received considerable attention [2]. This has led to the new field of nanostructured materials. In view of the attractive properties observed in such nanostructures, numerous synthesis techniques are presently under development for the production of these materials in large quantities. These include gas condensation, ball milling, sol–gel techniques, spark erosion, etc. [2]. Our research efforts have been concerned with electrochemical synthesis using conventional direct current electrodeposition, pulse plating, electroless plating and co-deposition processes to produce nanocomposite materials [3]. Electrodeposition has many advantages over other nanoprocessing techniques, including (1) the potentially very large number of pure metals, alloys and composite systems which can be deposited with grain sizes less than 100 nm, (2) the low initial capital investment required to synthesize these materials, (3) high production rates, (4) few size and shape limitations, and (5) the relatively minor "technological barriers" to be overcome in transferring this technology from the research laboratory to existing electroplating and electroforming industries.

Although there are numerous reports in the literature on electrodeposits with ultrafine grain structure (e.g. [4]) no systematic studies on the synthesis of nanocrystalline materials by electro-deposition to optimize certain properties by introducing large volume fractions of grain boundaries and triple junctions into the material were published prior to 1989 [5, 6].

Over the past five years, we have particularly studied the synthesis, structure and properties of nanocrystalline nickel. We have already shown [7–13], that grain refinement of electroplated nickel into the nanometre range (< 40 nm) results in unique and, in many cases, improved properties as compared to conventional polycrystalline nickel. For example, the hardness of electrodeposited nickel initially increases linearly far into the nanocrystalline range from the hardness of about 150 kg mm^{-2} for deposits with 100 μm grain size to about 650 kg mm^{-2} at 10 nm [7]. However, starting at grain sizes less than 30 nm, a clear deviation from the regular Hall–Petch relationship [14, 15] is observed leading to a plateau in the hardness curve at about 650 kg mm^{-2} for the smallest grain size of 10 nm. Thermal stability measurements at 573 K of electrodeposits with 10 nm grain size showed an initial rapid grain coarsening by a factor of approximately 2–3, before grain size stabilization occurred [8]. Potentiodynamic testing of nanocrystalline nickel electrodeposits in $2NH_2SO_4$ showed the regular active–passive–transpassive behaviour that is common for normal crystalline nickel [9]. Although

0022–2461

TABLE I Composition and pH of electroplating baths used in the present study

	($g l^{-1}$)
$Ni_2SO_4 \cdot 7H_2O$	300
$NiCl_2 \cdot 6H_2O$	45
Boric acid	45
Saccharin	0.5–10
pH adjusted to 2.0 with 7:1 ratio H_2SO_4:HCl acid mixture	

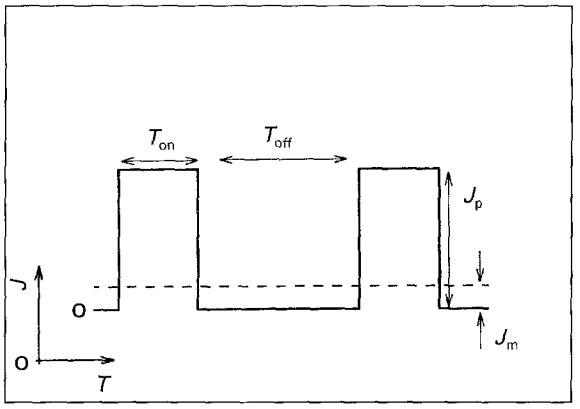

Figure 1 Schematic representation of pulse plating waveform showing the important pulse parameters: J_m; average current density; J_p, peak current density, T_{on}, pulse duration; T_{off}; pulse off-time.

TABLE II Pulse plating conditions leading to acceptable nanocrystalline nickel deposits from saccharin-containing Watts-type baths [17,18]

Parameter	Optimum value
On-time (ms)	2.5
Off-time (ms)	45
Peak current density ($mA cm^{-2}$)	1900
Temperature (°C)	65
pH	2.0

the overall dissolution rates in the passive range were somewhat enhanced in nanoprocessed material, it was found that nanocrystalline nickel exhibits superior resistance to localized corrosion [9]. Magnetic measurements showed that the saturation magnetization

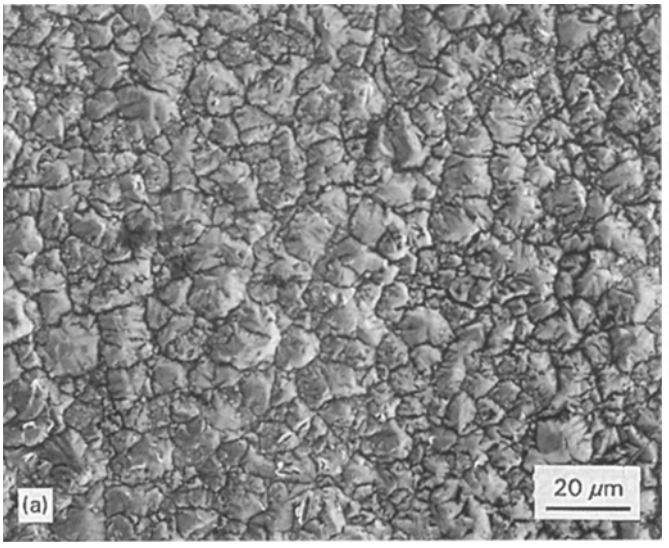

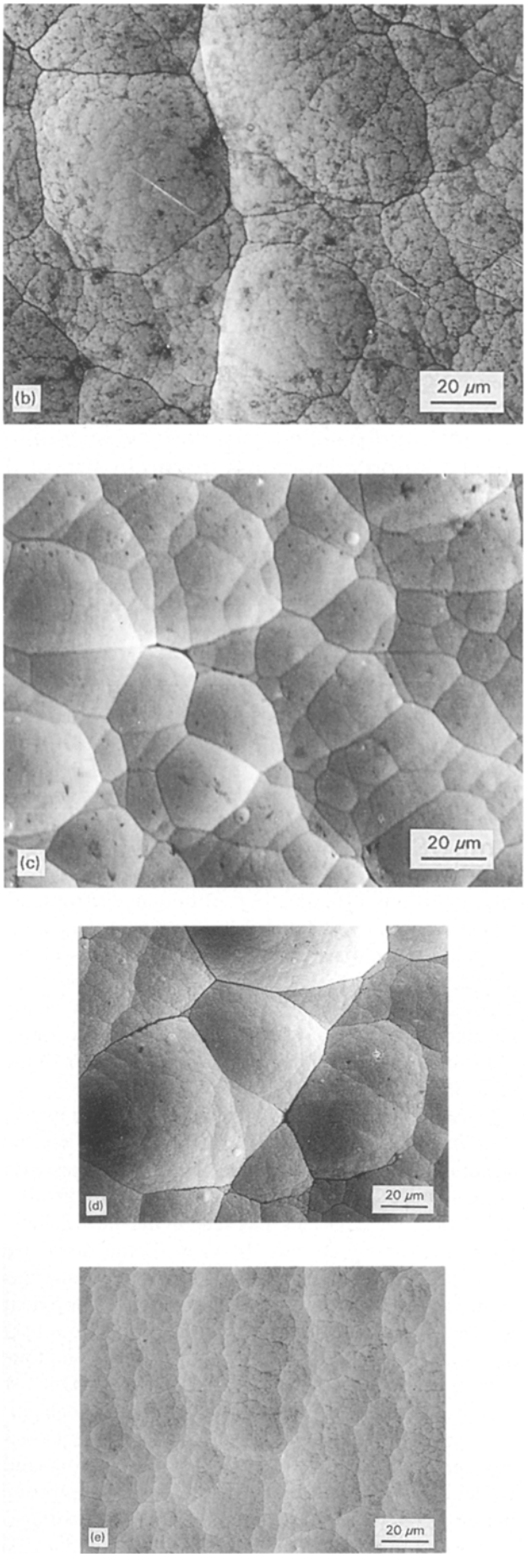

Figure 2 Influence of saccharin concentration in the bath on surface morphology of 300 μm thick nickel deposits with T_{on} of 2.5 ms, T_{off} of 45 ms and J_p of 1900 $mA cm^{-2}$: (a) 0.0 $g l^{-1}$; (b) 0.5 $g l^{-1}$; (c) 2.5 $g l^{-1}$; (d) 5 $g l^{-1}$ and (e) 10 $g l^{-1}$.

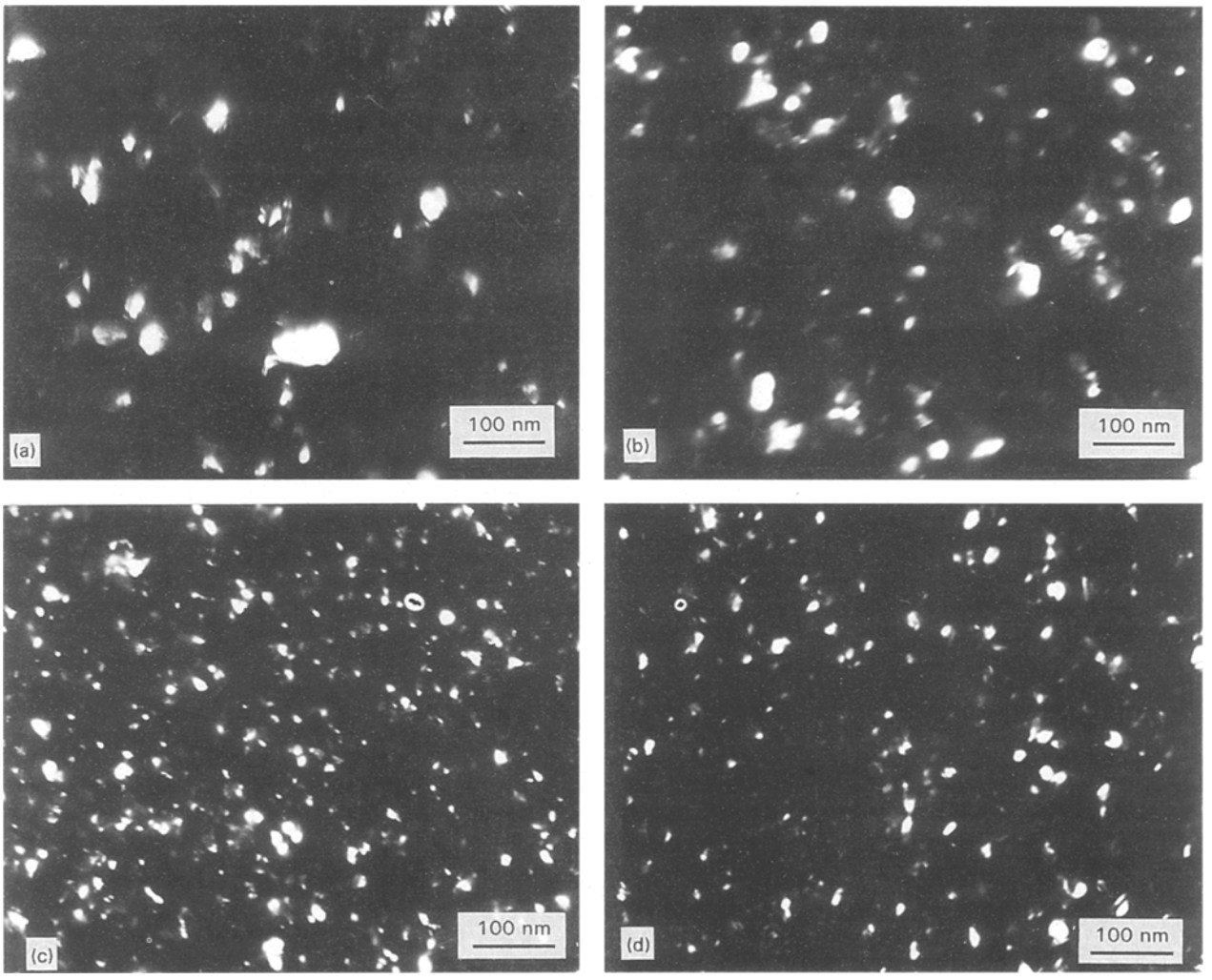

Figure 3 Dark-field electron micrographs showing the influence of saccharin concentration in the bath on the grain size of nickel deposits produced with T_{on} of 2.5 ms, T_{off} of 45 ms and J_p of 1900 mA cm^{-2}: (a) 0.5 g l^{-1}; (b) 2.5 g l^{-1}; (c) 5 g l^{-1} and (d) 10 g l^{-1}.

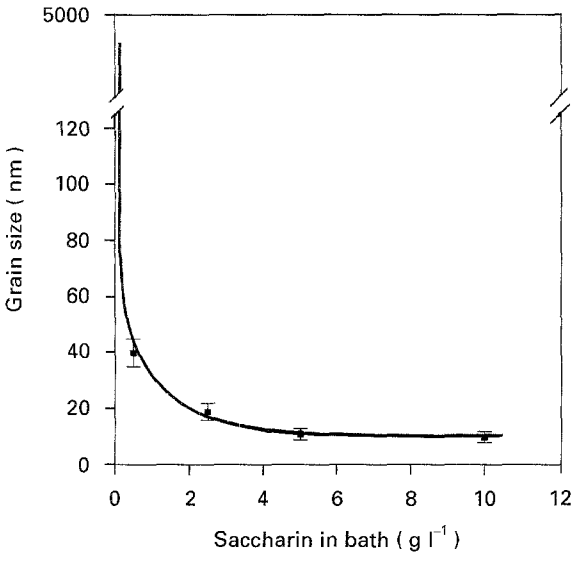

Figure 4 Grain size as a function of saccharin concentration in the bath of nickel deposits produced at (■) $T_{on} = 2.5$ ms, $T_{off} = 45$ ms, $J_p = 1900$ mA cm^{-2} and pH $\approx$ 2.0.

is little affected by the grain size of the nanocrystalline nickel down to grain sizes of 10 nm [10]. Nanocrystalline nickel deposits with a grain size of 10 nm also exhibited a three-fold increase in the room-temperature dc electrical resistivity as compared with conventional coarse-grained nickel which was explained in terms of electron scattering events at grain boundaries [11]. Hydrogen permeation studies on nanocrystalline nickel with a grain size of 17 nm yielded enhanced hydrogen diffusion coefficients for the grain- boundary and triple- junction components of the material [12]. Moreover, nanocrystalline nickel with a grain size of about 20 nm showed an 18-fold increase in the hydrogen solubility as compared to its conventional polycrystalline counterpart [13].

The purpose of the present paper is to present the details of the pulse electrodeposition technique used to synthesize these materials from a modified Watts' bath. The effects of the electrodeposition variables and the saccharin concentration in the bath on surface morphology, grain size and preferred orientation will be discussed.

2. Experimental procedure

Watts-type baths containing saccharin, as shown in Table I, in a standard 2l reaction kettle, were used to produce up to 300 μm thick nanocrystalline nickel electrodeposits. Analytical grade chemicals and distilled water were used to prepare the solutions. The solution temperature was maintained at 65 ± 0.1 °C

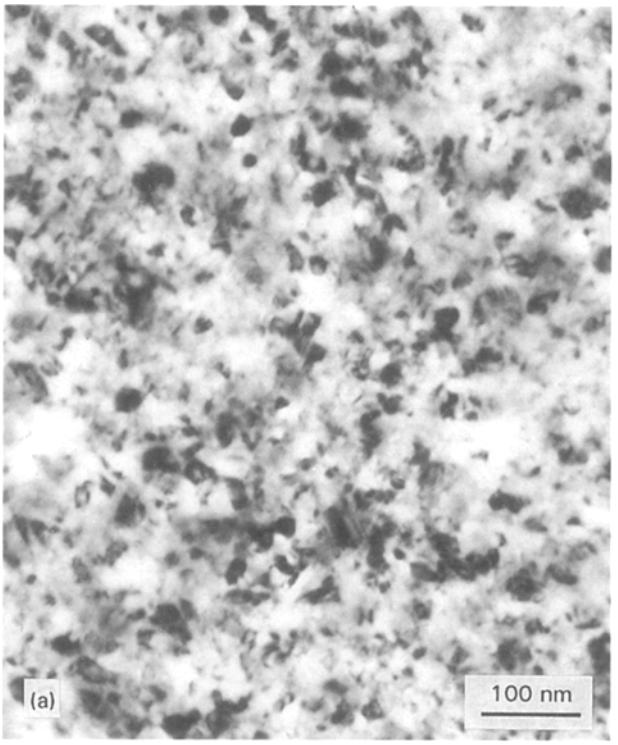

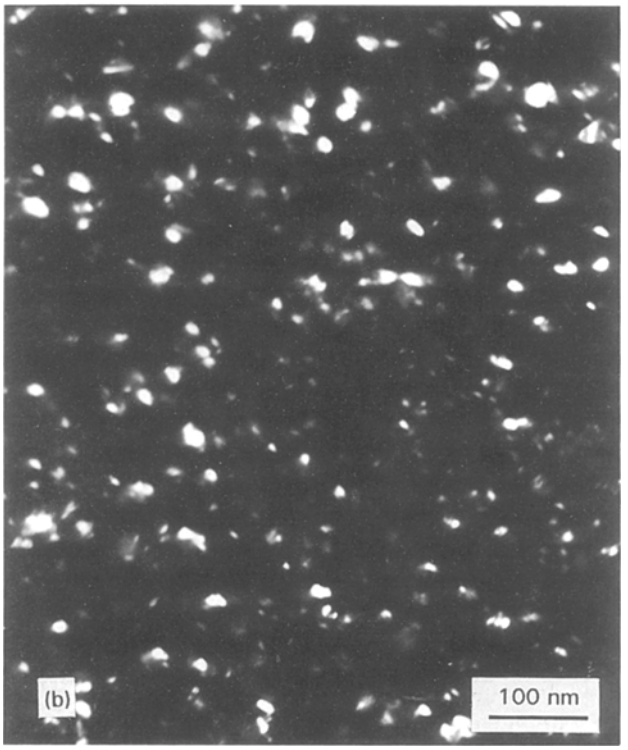

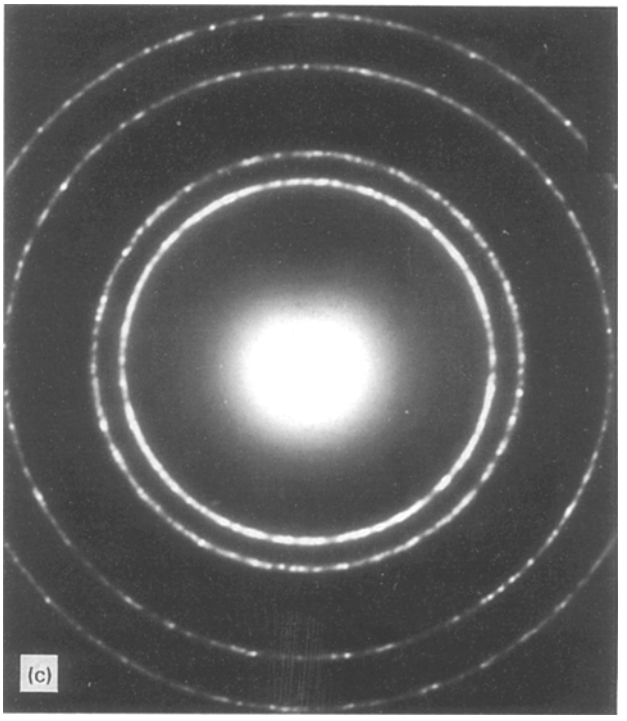

Figure 5 (a) Bright-field, (b) dark-field and (c) electron diffraction pattern of nanocrystalline nickel deposit produced at $T_{on} = 2.5$ ms, $T_{off} = 45$ ms, $J_p = 1900\,mA\,cm^{-2}$, pH ≈ 2.0 and $5\,g\,l^{-1}$ saccharin in the bath.

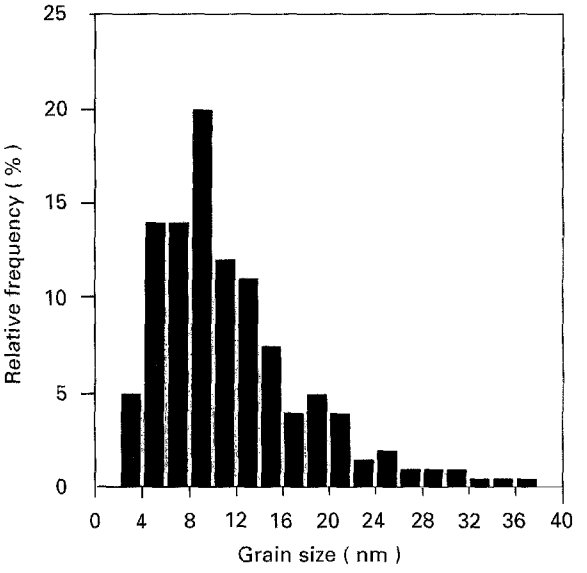

Figure 6 Grain-size distribution of nanocrystalline nickel deposit shown in Fig. 5.

by immersing the plating cell in a large volume thermostatted water bath. The saccharin concentration in the solution was changed in the sequence 0.5, 2.5, 5–10 $g\,l^{-1}$. Saccharin in the form of a powder was added to the plating bath and stirred until complete dissolution was achieved prior to the commencement of plating.

A high-purity (99.99 %) electrolytic nickel sheet contained in a titanium mesh basket was used as the soluble anode. Its surface area was approximately ten times greater than that of the cathode to ensure that there were no problems arising from anode polarization, particularly at high current densities [16]. The cathode substrate was made of titanium sheet with an exposed surface area of 1 or $2\,cm^2$. The anode was placed a distance of 8 cm away from the cathode. After electrodeposition, the nickel deposits were mechanically stripped off the titanium cathode.

Pulsed electrodeposition of nickel was carried out galvanostatically using cathodic square wave pulses with complete current cut-off during the interval between the pulses, as shown in Fig. 1. The optimum pulse plating parameters leading to acceptable deposits are shown in Table II [17, 18].

Scanning electron microscopy was used for the observation of the surface morphology of the as-plated

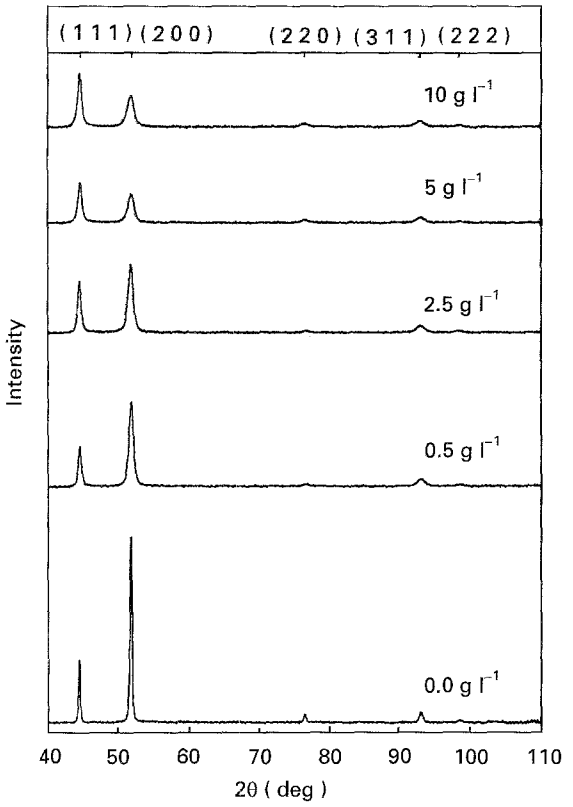

Figure 7 XRD patterns showing the influence of saccharin concentration in the bath on the preferred orientation of nickel deposits with $T_{on} = 2.5$ ms, $T_{off} = 45$ ms, $J_p = 1900\,mA\,cm^{-2}$.

surface of the electrodeposits. Bright-field and dark-field transmission electron micrographs were taken for the examination of the structure and grain size of nanocrystalline deposits. Thin foils for TEM examination were prepared by electropolishing using an electrolyte comprising 6% perchloric acid, 15% methanol and 79% acetic acid at a temperature of $-10\,°C$ and a voltage of 15 V d.c. The grain size of the nanocrystalline electrodeposits was determined directly from dark-field transmission electron micrographs by measuring approximately 250 grains. X-ray diffraction patterns were obtained using CuK_α radiation ($\lambda = 0.154\,184$ nm) on a standard θ–2θ diffractometer. Sulphur and carbon analyses of the deposits were carried out using the infrared absorption technique. Three nickel electrodeposits were used to obtain average analyses.

3. Results and discussion

Fig. 2 shows the surface morphology of nickel electrodeposits obtained at varying saccharin concentrations added to the plating bath. It is obvious that in the absence of saccharin (Fig. 2a) large crystals in the micrometre range are obtained. These deposits also exhibit relatively large surface roughness and dull appearance. A saccharin concentration of $0.5\,g\,l^{-1}$ resulted in a transition to a colony-like morphology with smoother surface roughness, brighter appearance and much smaller grain size. Similar surface morphologies were obtained with further increase in saccharin additions (Fig. 2c–e). This observation is consistent with the work conducted by Dennis and Fuggle [19, 20] on d.c.-plated nickel from organic additive-

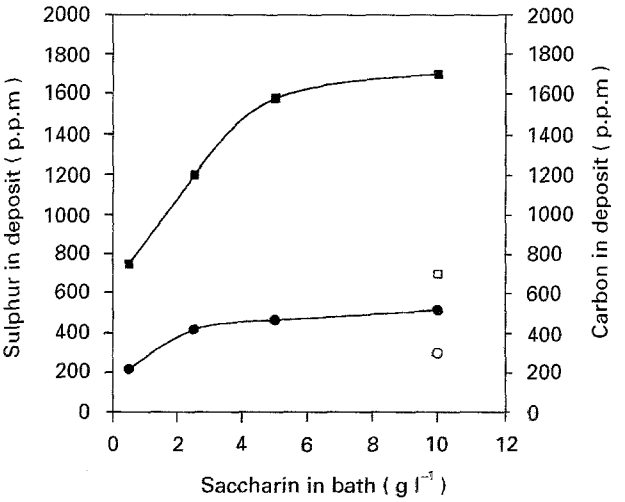

Figure 8 (■, □) Sulphur and (●, ○) carbon impurity contents in the deposit versus saccharin in bath for nickel deposits produced with T_{on} of 2.5 ms, T_{off} of 45 ms and J_p of $1900\,mA\,cm^{-2}$: (■, ●) pH ≈ 2.0 and (□, ○) pH ≈ 4.5.

containing Watts baths. These authors concluded that the incorporation of organic additives into the plating bath resulted in the inhibition of pyramidal growth and a concomitant reduction in surface roughness and increase in surface brightness. Weil and Cook [21] also reported the formation of colony-like morphology similar to that observed in Fig. 2a–e, when small amounts of coumarin or thiourea were added to the nickel plating solution. More recently, Nakamura *et al.* [22] observed similar morphological transitions in nickel electrodeposited from a Watts bath containing saccharin. These authors [21, 22] also reported a reduction in grain size in nickel electrodeposits produced from coumarin- or thiourea- [21], or saccharin- [22] containing baths, although no detailed grain size analysis was carried out.

TEM dark-field images (Fig. 3a–d) of the nickel deposits produced with saccharin concentrations in the range $0.5–10\,g\,l^{-1}$ show considerable changes in grain size. Increasing the saccharin concentration in the bath resulted in a progressive decrease in grain size. Fig. 4 is a graph showing the variation in deposit grain size with increasing saccharin concentrations in the bath. The grain size values plotted in this figure represent the 95% standard deviation value for approximately 250 grains counted directly from dark-field micrographs. It is evident from this figure that initially the grain size decreases rapidly with increasing saccharin additions before levelling off at saccharin concentrations of $5\,g\,l^{-1}$ and higher. Increasing the saccharin concentration in the bath from $5\,g\,l^{-1}$ to $10\,g\,l^{-1}$ has little effect on the grain size reduction. The ability of saccharin to refine the grain size is likely due to the combined effects of (1) lowering the overpotential for nickel ion reduction [22], (2) increasing the frequency of nucleation by blocking crystalline growth [23] and (3) retarding surface diffusion of nickle adatoms on the cathode surface [24].

The levelling off in grain-size reduction with increasing saccharin concentration (see Fig. 4) may be due to a corresponding levelling off in the overpotential and/or saturation of adsorption sites at the

cathode surface by saccharin molecules above a certain saccharin concentration. This is in agreement with the work of Roth and Leidheiser [25] who found that saccharin yielded overpotential curves which reached a plateau with increasing saccharin concentration in the bath. Saturation of adsorption sites on the cathode surface by saccharin was also reported by Edwards [26] with increased saccharin levels in the bath.

Fig. 5a–c show bright-field, dark-field and electron diffraction pattern, respectively, for a nickel deposit with an average grain size of 10 nm produced from a bath containing 5 $g l^{-1}$ saccharin. It is clear from the bright-field and dark-field micrographs that these nanocrystalline nickel electrodeposits (Fig. 5) have uniform structure and negligible porosity as confirmed by density measurements [27]. Another important feature of this structure is that some of the larger bright areas in the dark-field micrograph (Fig. 5b) actually consist of a number of smaller grains in similar orientation, indicating the presence of a microtexture over short distances. The grain-size distribution for this deposit shown in Fig. 6 can be approximated by a logarithmic-normal distribution with a much smaller width than observed in conventional polycrystalline materials [28].

The influence of saccharin additions on the preferred orientation of these nickel deposits is illustrated in Fig. 7. It can be seen from this figure that an increase in the saccharin concentration in the bath leads to a progressive change in the preferred orientation from a strong (2 0 0) fibre texture to a (1 1 1) (2 0 0) double fibre texture. This result is in agreement with the observations reported by Nakamura *et al.* [22] on the preferred orientation of d.c.-plated nickel from a Watts bath containing saccharin. In addition to changes in the preferred orientation, higher saccharin concentrations in the bath resulted in wider peaks indicative of smaller grain size which is in agreement with the results from the electron microscopy study.

Fig. 8 shows the variations of the sulphur and carbon impurity contents in the deposit with increasing saccharin concentration in the plating bath. The impurity content values plotted in this figure are the average of three assays. With increasing saccharin additions, initially both impurities increase rapidly before reaching a plateau at higher saccharin levels. Similar results have been reported by Edwards [26] and also Bonino *et al.* [23] during d.c. electrodeposition of nickel from saccharin-containing Watts baths. Moreover, Fig. 8 shows that at the same saccharin level, the sulphur content in the deposit is approximately three to four times higher than the carbon content.

For comparison purposes, the sulphur and carbon assay values for deposits produced from a bath containing 10 $g l^{-1}$ saccharin but at pH of 4.5 are also included in this figure. It can be seen that increasing the solution pH leads to a considerable decrease in the impurity content of the deposit. This is consistent with the work reported by Gill [29] and Brown [30] on the effect of pH on the co-deposition of sulphur from sulphur-bearing compounds added to nickel plating solutions.

4. Conclusion

This paper demonstrates that relatively pure ($\geq 99.5\%$) bulk nanocrystalline nickel deposits having grain sizes in the range 40–10 nm can be produced by pulse electrodeposition from saccharin-containing Watts-type baths. Increasing saccharin concentration in the plating bath resulted in an initial rapid decrease in grain size. Further reduction in grain size with increasing saccharin concentration beyond 5 $g l^{-1}$ was not observed. The electrodeposits produced by this method are smooth and exhibit high brightness. The preferred orientation of the deposits was found to change progressively from a (2 0 0) fibre texture at the lowest saccharin concentration of 0.5 $g l^{-1}$ to a (1 1 1) (2 0 0) double fibre texture at a saccharin concentration of 10 $g l^{-1}$. These deposits exhibit a narrow logarithmic-normal grain-size distribution.

Acknowledgements

The authors acknowledge stimulating discussions with Drs J. Page, G. Palumbo and K. T. Aust. Financial support from the Natural Sciences and Engineering Research Council of Canada, Energy, Mines and Resources of Canada and the School of Graduate Studies at Queen's University is gratefully acknowledged.

References

1. S. KAJA, H. W. PICKERING and W. R. BITLER, *Plat. Surf. Fin.* **72** (1986) 58.
2. H. GLEITER, *Progr. Mater. Sci.* **33** (1989) 223.
3. U. ERB, A. M. EL-SHERIK, G. PALUMBO and K. T. AUST, *Nanostr. Mater.* **2** (1993) 383.
4. A. BRENNER, "Electrodeposition of Alloys-Principles and Practice" (Academic Press, New York, 1963).
5. G. MĆMAHON and U. ERB, *Microstr. Sci.* **17** (1989) 447.
6. *Idem, J. Mater. Sci. Lett.* **8** (1989) 865.
7. A. M. EL-SHERIK, U. ERB, G. PALUMBO and K. AUST, *Scripta Metall. Mater.* **27** (1992) 1185.
8. A. M. EL-SHERIK, K. BOYLAN, U. ERB, G. PALUMBO and K. AUST, *MRS Symp. Proc.* **238** (1992) 727.
9. R. ROFAGHA, R. LANGER, A. M. EL-SHERIK, U. ERB, G. PALUMBO and K. AUST, *Scripta Metall. Mater.* **25** (1991) 2867.
10. M. J. AUS, B. SZPUNAR, A. M. EL-SHERIK, U. ERB, G. PALUMBO and K. AUST, *ibid.* **27** (1992) 1639.
11. M. J. AUS, B. SZPUNAR, U. ERB, A. M. EL-SHERIK, G. PALUMBO and K. AUST, *J. Appl. Phys.* **75** (1994) 3632.
12. G. PALUMBO, D. M. DOYLE, A. M. EL-SHERIK, U. ERB and K. AUST, *Scripta Metall. Mater.* **25** (1991) 679.
13. D. M. DOYLE, G. PALUMBO, K. T. AUST, A. M. EL-SHERIK, and U. ERB *Acta. Metall. Mater.*, **43** (1995) 3027.
14. O. E. HALL, *Proc. Phys. Soc. Lond.* **B64** (1951) 747.
15. N. J. PETCH, *J. Iron Steel Inst.* **25** (1953) 174.
16. N. V. PARTHASARADHY, "Practical Electroplating Handbook" (Prentice Hall, Englewood Cliffs, NJ, 1989).
17. A. M. EL-SHERIK, PhD thesis, Queen's University, Kingston, Ontario (1993).
18. U. ERB and A. M. EL-SHERIK, "Nanocrystalline Metals and Process of Producing the same," US Pat. 5, 352, 266, 1994.
19. J. K. DENIS and J. J. FUGGLE, *Electroplat. Metal Fin.* **20** (1967) 370.
20. *Idem, ibid.* **21** (1968) 16.
21. R. WEIL and H. C. COOK, *J. Electrochem. Soc.* **109** (1962) 295.

22. Y. NAKAMURA, N. KANEKO, M. WATANABE and H. NEZU, *J. Appl. Electrochem.* **24** (1994) 227.
23. J. P. BONINO, P. POUDEROUX, C. ROSSIGNOL and A. ROUSSET, *Plat. Surf. Fin.* **78** (1992).
24. R. T. C. CHOO, J. TOGURI, A. M. EL-SHERIK and U. ERB, *J. Appl. Electrochem.*, **25** (1995) 384.
25. C. C. ROTH and H. LEIDHEISER Jr, *J. Electrochem. Soc.* **100** (1953) 553.
26. J. EDWARDS, *Trans. Inst. Metal Fin.* **41** (1964) 169.
27. T. HAASZ, BSc thesis, University of Toronto, Toronto, Ontario (1993).
28. J. LIAN, B. BAUDELET and A. A. NAZAROV, *Mater. Sci. Eng.* **A172** (1993) 23.
29. K. S. GILL, PhD thesis, Queen's University, Kingston, Ontario (1990).
30. H. BROWN, *Plating* **55** (1968) 1047.

Received 16 May 1994
and accepted 17 May 1995